A bio-inspired expandable soft suction gripper for minimal invasive surgery—an explorative design study

Kortman, Vera G.; Sakes, Aimée; Endo, Gen; Breedveld, Paul

DOI
10.1088/1748-3190/accd35

Publication date
2023

Document Version
Final published version

Published in
Bioinspiration and Biomimetics

A bio-inspired expandable soft suction gripper for minimal invasive surgery—an explorative design study

IOP Publishing Bioinspir. Biomim. 18 (2023) 046004 https://doi.org/10.1088/1748-3190/accd35

Bioinspiration & Biomimetics

OPEN ACCESS

RECEIVED
18 January 2023

REVISED
10 March 2023

ACCEPTED FOR PUBLICATION
12 April 2023

PUBLISHED
10 May 2023

PAPER

A bio-inspired expandable soft suction gripper for minimal invasive surgery—an explorative design study

Vera G Kortman[1,*], **Aimée Sakes**[1], **Gen Endo**[2] **and Paul Breedveld**[1]

[1] Bio-Inspired Technology Group (BITE), Department BioMechanical Engineering, Faculty of Mechanical, Maritime, and Materials Engineering, Delft University of Technology, 2628 CD Delft, The Netherlands
[2] Department of Mechanical Engineering, Tokyo Institute of Technology, Tokyo, Japan
[*] Author to whom any correspondence should be addressed.

E-mail: V.G.Kortman@tudelft.nl

Keywords: suction cup, vacuum grasper, bio-inspiration, biomimicry, octopus, soft robotics, medical device

Supplementary material for this article is available online

Abstract

Gripping slippery and flexible tissues during minimal invasive surgery (MIS) is often challenging using a conventional tissue gripper. A force grip has to compensate for the low friction coefficient between the gripper's jaws and the tissue surface. This study focuses on the development of a suction gripper. This device applies a pressure difference to grip the target tissue without the need to enclose it. Inspiration is taken from biological suction discs, as these are able to attach to a wide variety of substrates, varying from soft and slimy surfaces to rigid and rough rocks. Our bio-inspired suction gripper is divided into two main parts: (1) the suction chamber inside the handle where vacuum pressure is generated, and (2) the suction tip that attaches to the target tissue. The suction gripper fits through a ∅ 10 mm trocar and unfolds in a larger suction surface when being extracted. The suction tip is structured in a layered manner. The tip integrates five functions in separate layers to allow for safe and effective tissue handling: (1) foldability, (2) air-tightness, (3) slideability, (4) friction magnification and (5) seal generation. The contact surface of the tip creates an air-tight seal with the tissue and enhances frictional support. The suction tip's shape grip allows for the gripping of small tissue pieces and enhances its resistance against shear forces. The experiments illustrated that our suction gripper outperforms man-made suction discs, as well as currently described suction grippers in literature in terms of attachment force (5.95 ± 0.52 N on muscle tissue) and substrate versatility. Our bio-inspired suction gripper offers the opportunity for a safer alternative to the conventional tissue gripper in MIS.

1. Introduction

1.1. Surgical grippers versus suction grippers

Gently but securely gripping and handling of slippery, compliant and irregular tissues remains one of the most challenging procedures during minimal invasive surgery (MIS). In MIS, slender instruments are guided into the abdomen via trocars. These trocars act as portals through small incisions (figure 1(a)). They typically have a diameter between 5 and 10 mm. Grippers used in current practice commonly use a force grip to manipulate tissues. This force grip is applied by two jaws that grip the tissues sideways and is subsequently translated into a pull force, to relocate or stretch the gripped tissue (figure 1(b)) [1]. To prevent slip and to compensate for the low friction coefficients between the jaws and tissue, high pinch forces are often applied [2], which in turn can lead to unwanted tissue trauma [1, 3, 4]. Furthermore, force feedback is limited in the currently available MIS grippers, thus creating the risk of excessive force application during surgery and unintended tissue injury.

Tissue trauma due to excessive clamping forces of the gripper can lead to severe implications [1–3, 5]. Bowel perforation is an example of an implication with a high mortality rate due to improper gripper use [6]. Furthermore, Joice *et al* [7] showed that the largest number of surgical errors during gall bladder removal is associated with gripper jaw induced tearing of the tissue. Next to the bowel and gall bladder, the bile duct, ureters, fallopian tubes and spleen are examples of delicate organs prone to damage by gripping [8].

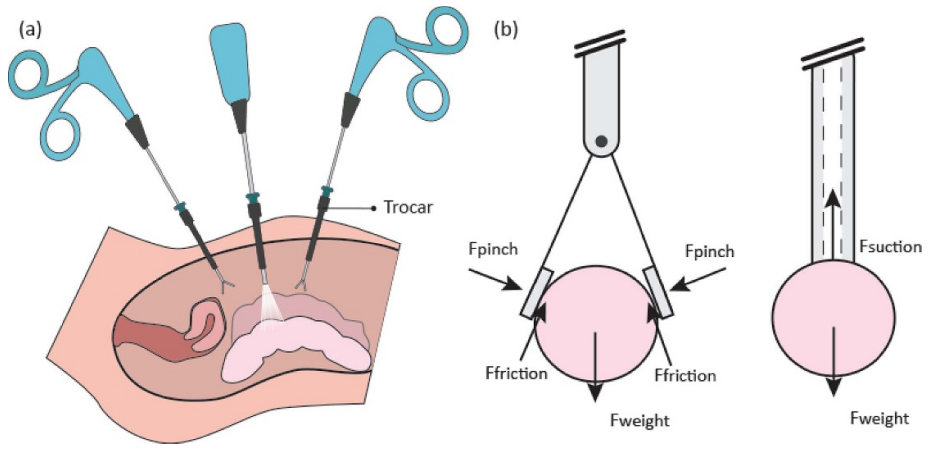

Figure 1. (a) Schematic overview of a minimally invasive procedure accessing the abdomen. (b) Overview of the forces acting on tissue by a grasping forceps (left) and a suction gripper (right).

In order to overcome these challenges, a new type of gripper can be introduced that does not need to enclose the tissue in order to apply high pinch forces for sufficient grip. An interesting direction for this challenge is suction attachment, in which a pressure differential is used to grip different substrates (figure 1(b)). Suction grippers can exert pull forces directly in line with the instrument shaft, which limits damage caused by compressive pinch forces from the sides. This makes suction technology not only potentially relevant for gripping delicate and slippery tissue, but also for gripping large organs that can not be clamped between the jaws of a grasping forceps.

1.2. State of the art

Suction grippers are widely used in industry to grasp a variety of objects, such as cardboard packages, sheet metal, bottles or electronic components. In the medical field, however, commercially available suction stabilizers only exist for (open) cardiac surgery. Examples are the *Octopus Heart Stabilizer* (Medtronic), the *Starfish* (Medtronic) and the *Xpose 3* (Getinge). These devices have been designed to locally stabilize heart tissue during off-pump coronary artery bypass surgery [9–12]. Next to these commercially available devices, suction grippers are described in literature for tissue stabilization, drug delivery and tissue dissection [13–15]. In addition, suction discs have been successfully tested *in vivo* as a locomotion strategy on heart tissue to perform injections in the heart wall [16, 17].

The devices mentioned above clearly show the potential of suction technology to interact with tissue in MIS. However, the forces that these devices can exert are relatively low, in the range of 1 N, and thus do not allow for tissue lifting or stretching. Only two suction grippers specifically designed for tissue manipulation during MIS have been identified in literature: (1) a laparoscopic suction gripper for bowel manipulation (developed at Delft University of Technology) [18] and (2) a lung positioner for thoracoscopic surgery (developed at Tokyo institute of technology) [19]. The laparoscopic suction gripper consists of a rigid suction nozzle and was able to generate an attachment force of 5.6 N on bowel tissue using a vacuum pressure of 80 kPa [18]. The lung positioner consists of an array of rigid suction chambers that form a triangular shape inside the body after insertion through a small incision [19]. Even though both devices showed that suction technology is promising for tissue manipulation in a minimally invasive setting, they were challenging to manufacture and vulnerable to air leaks. This vulnerability was substantiated by the lung positioner requiring a continuous vacuum inflow in order to maintain grip on the tissue [19]. Therefore, further development in terms of grip, substrate diversity and manufacturing is needed to bring the concept of vacuum gripping during MIS to the operating room.

1.3. Inspiration from biological suction discs

Rubber suction discs are commonplace in our daily environment. Unfortunately, the possibilities of suction attachment of current man-made suction discs are still limited since these discs do not adhere to rough substrates with a roughness greater than 35 μm (where roughness is defined as the average grain size) [21], or remain stationary on slippery substrates when subjected to external forces. This is mainly due to their inability to create a sufficient seal or sufficient friction between the disc and the substrate, making them less suited for attachment to rough surfaces and slippery and soft tissues. Also, the suction attachment of these discs is dependent on deformation due to an initial pressing force, which is undesired for applications on tissues during surgery.

In a number of scientific research groups in the world, research is being carried out unraveling the working mechanisms of suction discs found in

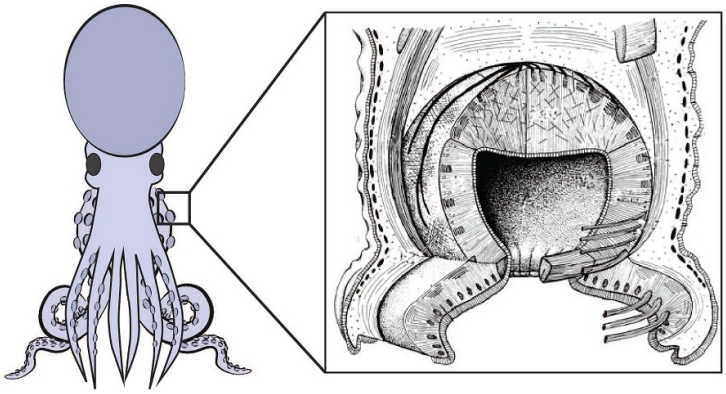

Figure 2. Schematic overview of the suction disc of the *Octopod Vulgaris*. Reproduced with permission from [20]. © 2002, Oxford University Press.

nature, as these outperform man-made suction discs in terms of versatility [22]. Many biological suction discs are able to attach to a wide range of substrates, varying from soft and slimy surfaces to rigid and rough rocks [21, 23]. Examples of animals with such powerful suction discs are clingfish, octopods, aquatic insect larvae and starfish [23–28] (figure 2). The process of attachment and detachment can be quite dynamic, with some gobiidae fish able to climb the vertical cliffs of waterfalls using a pelvic-fin-derived suction disc [29]. Hill-stream loaches even use their entire body as sucker for anchoring in high-speed flows in stream environments [30, 31].

Researchers reported varying ways to design bio-inspired suction discs. The main focus of current research efforts is on mimicking the material characteristics and morphology of the suction disc rim to enable improved attachment performance, for example used for fruit handling in industry. It must be noted that none of these bio-inspired discs has been developed specifically for MIS. Tramacere *et al* [32] developed octopod inspired suction discs made of soft elastomeric materials and with a network of grooves on their surface. Ditsche and Summers [21] and Sandoval *et al* [33] developed suction discs inspired by the northern clingfish that featured highly elastic contact surfaces, various types of inclusions, slits and bio-inspired body geometry. Sadeghi *et al* [34] developed a sucker pad inspired by the tube feet of sea urchins, where multiple individually sealed suction discs are actuated by one vacuum chamber. Designed for the manipulation of fragile, rough or wet objects, these studies evaluated the attachment performance of their bio-inspired suction discs on varying substrates compared to man-made suction discs. The results showed that the bio-inspired suction discs outperformed conventional man-made suction discs in terms of substrate diversity, as they were able to adhere to rough and wet substrates where man-made discs failed [21, 33].

1.4. Aim of this study

Even though major strides have been made in the development of bio-inspired suction discs, a number of challenges need to be researched and overcome for tissue manipulation in MIS, such as the generation of sufficient forces for tissue lifting and stretching while incorporating outer dimensions applicable for MIS and maintaining stable sealing. This study uses biological suction discs as inspiration to propose a novel design for a minimally invasive tissue gripper actuated by suction. We will investigate how nature is able to create a strong seal on soft surfaces and how to translate this into a small diameter soft suction disc design for MIS. The goal of our study is, therefore, to develop and test a bio-inspired suction gripper for manipulating flexible and slippery surfaces during MIS.

2. Analysis biological suction disc

2.1. Decoupling functions

In order to understand how man-made and biological discs differ from one another, the working principle of a regular man-made suction disc and an octopod suction disc is analyzed. Figure 3 visualizes this analysis in a stepwise manner. The first row shows how both suction disc types generally generate suction. An octopod suction disc has a clear distinction between a dedicated suction chamber that generates the vacuum force and an optimized contact surface that maintains the seal and increases grip generation, whereas man-made suction discs generally combine these functions in one single flexible component [20, 22, 26, 35–37].

2.2. Suction generation

In the design of regular man-made suction discs, the suction chamber is usually integrated with the contact surface. The deformation of this contact surface generates the suction force. The concave contact surface is pressed towards the substrate (F_i) to expel the

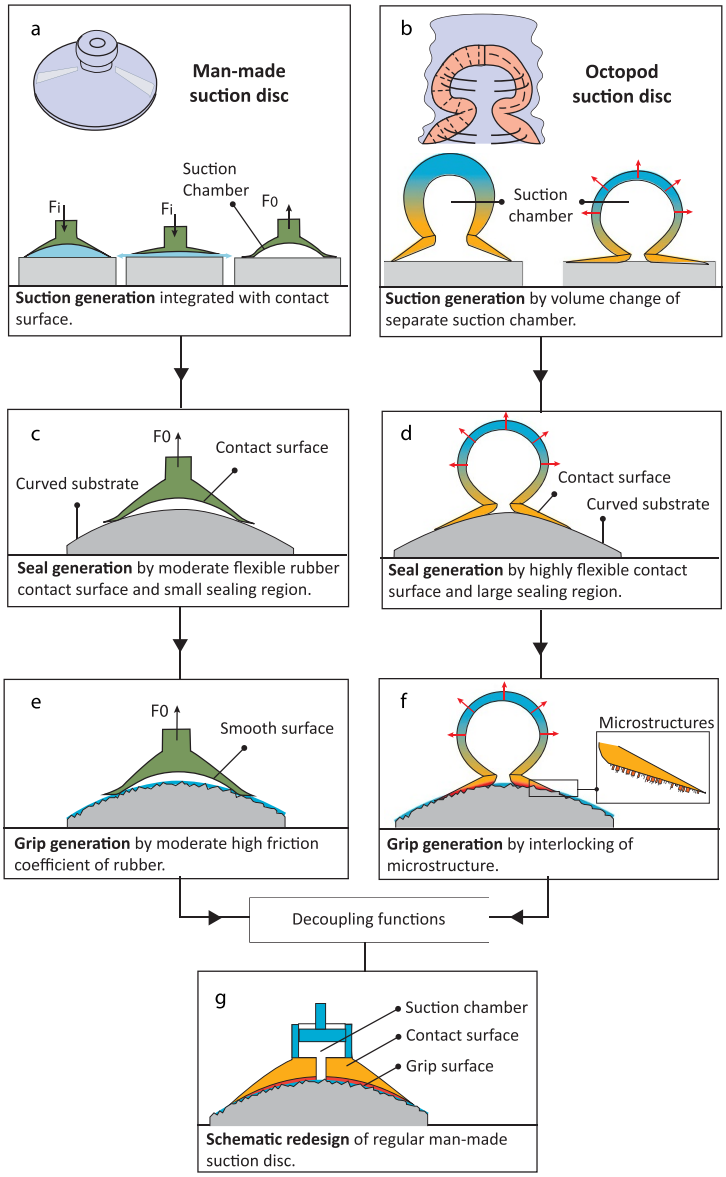

Figure 3. Improval of a regular man-made suction disc by looking at the functionality of the suction disc of an octopus. (a) Suction generation of a man-made suction disc. Here, (F_i) represents the initial pressing force and (F_0) the stiffness force of the disc. (b) Suction generation of an octopod suction disc. (c) Seal generation of the man-made suction disc. (d) Seal generation of the octopod suction disc. (e) Grip generation of the man-made suction disc. (f) Grip generation of the octopod suction disc. (g) Schematic redesign of the man-made suction disc by decoupling the functions in separate components. For a more detailed explanation, see text. Color indications: blue: suction generation, orange: seal generation, red: grip generation, grey: rigid substrate.

air between the two surfaces [38]. The stiffness force of the body of the suction disc (F_0), generated by its internal strain, tends to restore the original shape of the disc (figure 3(a)), which then generates the vacuum force [38, 39]. This means that a trade-off is made between the required stiffness of the disc to restore its original shape and the required flexibility of the disc to create a seal.

The suction chamber and the contact surface of an octopod suction disc are physically separated. Therefore, they are specialized for their own function, suction generation and seal- and grip generation, respectively. The shape, flexibility and musculature of the suction chamber are optimized for generating powerful volume change. The highly specialized musculature is subdivided into radial, circular and meridional muscles (figure 3(b)) [35, 37]. As the chamber acts as a muscular hydrostat, muscle contraction in one direction results in the elongation of a muscle in another direction [35, 37]. The suction chamber's wall thins by contraction of the radial muscles, which increases the internal volume of the suction chamber and results in a vacuum force. Cross connective fibers prevent the collapse of the suction chamber when being subjected to vacuum pressure [20]. This form of dimensional stability is also identified in

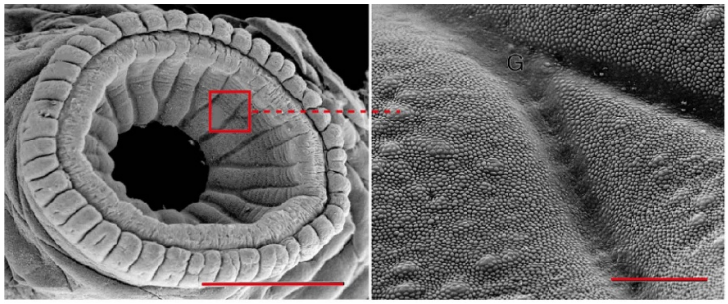

Figure 4. Scanning electron micrograph of the rim of the *Octopus Bimaculoides* sucker. Left: the contact surface of the suction disc is covered with grooves. Scale bar: 1.0 mm. Right: the contact surface is additionally covered with microstructures to provide frictional support. Scale bar: 100 μm. Reproduced with permission from [20]. © 2002, Oxford University Press.

the northern clingfish's suction disc, where collagen bundles and flexible rays in the suction chamber's wall add resistance against vacuum pressure [40, 41].

2.3. Seal generation

The contact surface of a regular man-made suction disc is usually unable to adapt sufficiently to curved or rough substrates, as the disc as a whole, including the part in contact with the substrate, requires a certain amount of stiffness for sufficient vacuum generation (figure 3(c)). Due to the physical separation of the suction chamber from the contact surface, the contact surface of an octopod suction disc can be optimized for its sealing properties (figure 3(d)) [42–44]. The contact surface of an octopod disc contains ridges and grooves that usually mold with the contours of the substrate, thereby closing leakage channels [20, 26]. The surface consists of a highly flexible material, allowing it to follow the curves and irregularities of the substrate. Tramacere *et al* [36] found that the contact surface of an octopod suction disc has a Young's modulus of 7.7 kPa, which is very low as compared to rubber with a Young's modulus between 1–10 MPa [45]. For this reason, an octopod suction disc is able to easily attach to curved and rough substrates. Furthermore, the radial muscles in the disc's contact surface are oriented in such a way that contraction results in flattening and enlargement of the contact surface [20]. This lowers the disc's susceptibility to leakage as it enables the increasing of the sealing region [42]. Tramacere *et al* tested the influence of suction cup flexibility by mimicking the structured suction disc's contact surface of octopi using Ecoflex 00-30 silicone (Smooth-On Inc. USA). This resulted in approximately 65% higher pull-off forces as compared to a regular suction disc [32].

2.4. Grip generation

Whereas the regular man-made suction disc generally contains a smooth contact surface (figure 3(e)), the contact surface of an octopod suction disc reveals microstructures (figure 3(f)) [22, 32]. These microstructures are also identified on suction discs of a number of other animal classes like decapods [20, 46], clingfish [21, 23, 24, 40], remoras [47, 48], lumpsuckers [41], river loaches [31], catfish [49–52], blepharicerid larvae [25, 53] and parasites [54]. They can appear as rigid hooks that extend from the skeleton, or flexible structures that extend from the epidermis [23, 24, 40, 47, 54]. The rigid hooks interlock with the asperities of the substrate, thereby acting as a ratchet system [48]. The flexible microstructures usually mold over the asperities of the substrate [44]. This increases the contact area between the suction disc and substrate and generates an interlocking effect, which both enhance the disc's grip [24, 31]. Figure 4 shows that the suction disc's contact surface of the *Octopus bimaculoides* is covered with grooves and protrusions. The radius of the protrusions is approximately 3–4 μm [46]. The microstructures on the contact surface of the Clingfish is even more hierarchically layered, where the smallest protrusions can adapt to surface asperities of just a few nanometers [21, 24]. These microstructures form a layer on top of the contact surface that magnifies its grip. The magnification of the grip enhances the resistance against shear forces and inward slip. This plays an essential role in the disc's attachment performance, as the man-made suction disc tends to slip inwards when it is pulled off, causing the seal to break rather easily [23, 31]. Also, the interlocking effect results in better grip on slippery surfaces.

2.5. Schematic disc design

A schematic redesign of a regular man-made suction disc had been made inspired by the decoupled functions in an octopod suction disc, which are suction generation, seal generation and grip generation (figure 3(g)). Here, suction generation and seal generation are similarly decoupled in a separate suction chamber that conducts volume change and in a dedicated flexible contact surface that creates a seal. By decoupling these functions, no trade-off has to be made between the required stiffness for the vacuum generation and the required flexibility for the seal generation. The contact surface is optimized to maximize the sealing region, which lowers the disc's susceptibility to leakage. The contact surface is reinforced

by a dedicated grip surface optimized on the magnification of grip counteracting shear stresses.

3. Prototype development

3.1. Design constraints

The schematic redesign of the regular man-made suction disc in the previous section acts as base for our suction gripper's design. Some additional design constraints are related to the gripper's use in MIS to ensure safe and reliable handling of slippery tissue. The vacuum force of the disc has a theoretical limit defined by its maximal suction surface and vacuum pressure. Our suction gripper will be actuated by a vacuum pressure of 50 kPa, as the use of this amount of vacuum pressure on human tissue has been extensively tested by the commercially available *Octopus Heart Stabilizer* (Medtronic) [10, 11, 55]. Higher vacuum pressures could risk tissue damage. Next to a fixed vacuum pressure, the space available as vacuum surface limits the maximum vacuum force further. The vacuum surface is constrained by the allowed dimensions for surgical instruments during MIS. The vacuum gripper should be guided into the body by a trocar with a maximal diameter of 10 mm, which defines the maximally allowed outer dimensions of the vacuum gripper. The maximum space for the suction surface, a circle 10 mm in diameter, with a maximum vacuum pressure of 50 kPa, results in a theoretical maximum vacuum force of only 3.9 N, assuming that the entire allowed space is used as suction surface, meaning that the wall thickness of the disc equals zero. To place this in perspective, a short literature survey was conducted to list the mass of the different organs inside the human body. Table 1 shows an overview of the weight of some of the largest organs, showing the need for roughly 50% higher vacuum forces for tissue lifting, depending on the organ. A strategy for higher vacuum force generation is integrating a folding mechanism into the suction disc, such that it unfolds into a larger suction surface when guided into the abdomen through the trocar.

Table 1. The weights of some of the largest organs.

Organ	Weight (g)
Prostate	34.6 ± 13.1 [56]
Pancreas	144 ± 39 [57]
Spleen	156 ± 87 [57]
Kidney	162 ± 39 [57]
Heart	365 ± 71 [57]
Right lung	569 ± 175 [58]

3.2. Design suction tip

3.2.1. Layered disc design

The octopod suction disc analysis in the previous section reveals that a regular man-made suction disc can be improved by separating its suction chamber and contact surface and optimizing these for their own function. We will first focus on the design of the suction tip of the suction gripper, which enhances seal generation and grip generation on slippery tissue. The design of the suction chamber is less critical, as there is much design freedom to integrate this chamber in the suction gripper, e.g. in the handle or the shaft of the device.

The suction tip's design integrates five functions that it needs to fulfil in order to allow for safe and effective tissue handling:

- Allow the suction tip to expand into a larger suction surface (foldability).
- Create an air-tight suction tip (air-tightness).
- Allow for a smooth transition of the suction tip through the trocar (slideability).
- Magnify the friction coefficient between the suction tip and tissue (friction magnification).
- Allow secure sealing region formation (seal generation).

These functions were translated into separate layers of the suction tip, see figure 5.

In order to expand the suction surface of the suction tip, a number of folding mechanisms were considered, varying in their way to transform from an unfolded into a folded state. The challenge was to integrate a mechanism with easy actuation, small required space and the ability to resist high vacuum pressures. A suction tip containing pre-bent rays proved most optimal. These flexible rays return to their natural bent shape after guidance through the trocar. This means that no external actuation is needed to transform the tip into its unfolded state, minimizing usage steps for the surgeon. Additionally, these rays act as a support structure that strengthens the tip's dimensional stability when its subjected to high vacuum pressures. Moreover, the tip maintains its overall flexibility which is needed for folding.

Leakage of the foldable suction tip was prevented by an air-tight layer that covered the folding mechanism. The challenge of this layer's design was to minimize its thickness while maintaining its air-tightness, easy manufacturing and providing a smooth integration with the folding mechanism. A thin layer of silicone turned out to act best considering silicone's high elongation rate, its ability for casting as a thin film and its bio-compatibility. The silicone was reinforced by a finely woven mesh, which acted as a base to cast the silicone film in a three-dimensional shape. The silicon layer interlocks between the mesh fibers after curing to create a secure bond. Also, the mesh provides additional dimensional stability, similar to the collagen fibers of the octopod's suction disc. The silicone enclosure was covered by a thin foil with a low friction coefficient with the trocar.

The design of the footprint of the suction tip was focused on the generation of a secure seal and the

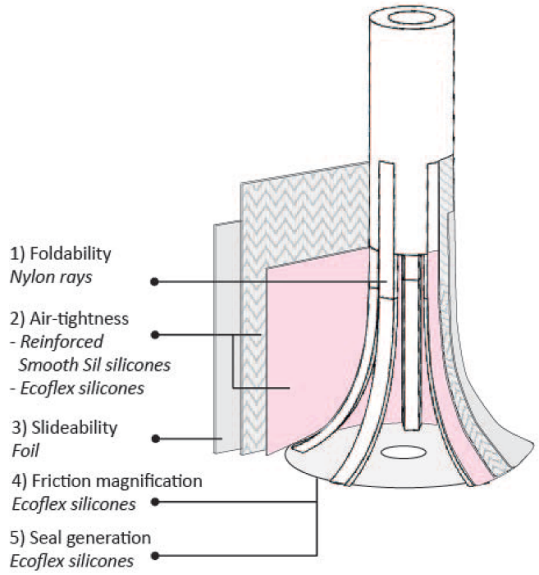

Figure 5. Final suction tip design. The final suction tip integrates five functions in separate layers. Pre-bent flat nylons rays act as a folding mechanism. A finely woven mesh serves as reinforcement for the Smooth Sil silicones. Together they provide an air-tight enclosing of the suction tip. A foil eases sliding through the trocar. The footprint layer consists of a membrane fabricated by Ecoflex silicones, which adds high frictional support with the tissue and supports sealing.

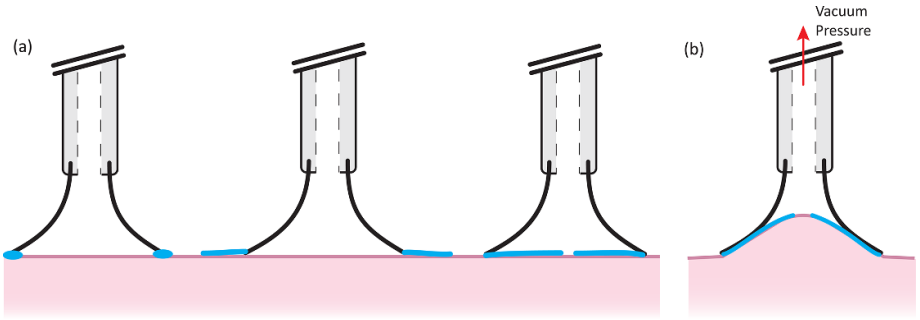

Figure 6. Footprint configurations (a) three footprint configurations with different sealing regions in blue. At the left, the edge of the suction tip covered by a flexible material, resulting in a small sealing region. In the middle, the suction tip with a flexible membrane on the outside, resulting in a large sealing region. At the right, the suction tip with a flexible membrane on the inside, resulting in a large sealing region and small occupied space. (b) When vacuum pressure is applied, the tissue is pressed onto the sealing region.

magnification of the friction coefficient with the surface of tissue. For the generation of a secure sealing region, the challenge was to lower the risk of the formation of leakage channels between the suction tip's footprint and tissue surface. This is achieved by attaching highly flexible material to the sturdy edge of the suction tip to make the tip better adaptable to the tissue surface. Figure 6(a) shows three possible footprint configurations of this flexible layer. The first configuration shows the suction tip with only its edge covered by flexible material, which creates short leakage channels that can result in failure. In the second configuration, a flexible membrane is attached to the outside of the tip's edge. Because of the membrane, atmospheric air has to intrude a longer distance before causing leakage. The downside of this second footprint configuration is the occupied space of the suction tip. This problem is avoided by placing the flexible membrane at the inside of the tip's edge, as shown in the third configuration. This configuration has the additional benefit that the tissue is pressed onto the footprint of the suction tip when the vacuum pressure pulls the tissue inside the tip (figure 6(b)). The flexible membrane incorporates a high friction coefficient with tissue to enhance the suction tip's frictional support against shear forces.

3.2.2. Intended use

The intended use of the suction gripper is visualized in figure 7. The gripper's tip unfolds after being guided into the abdomen through the trocar

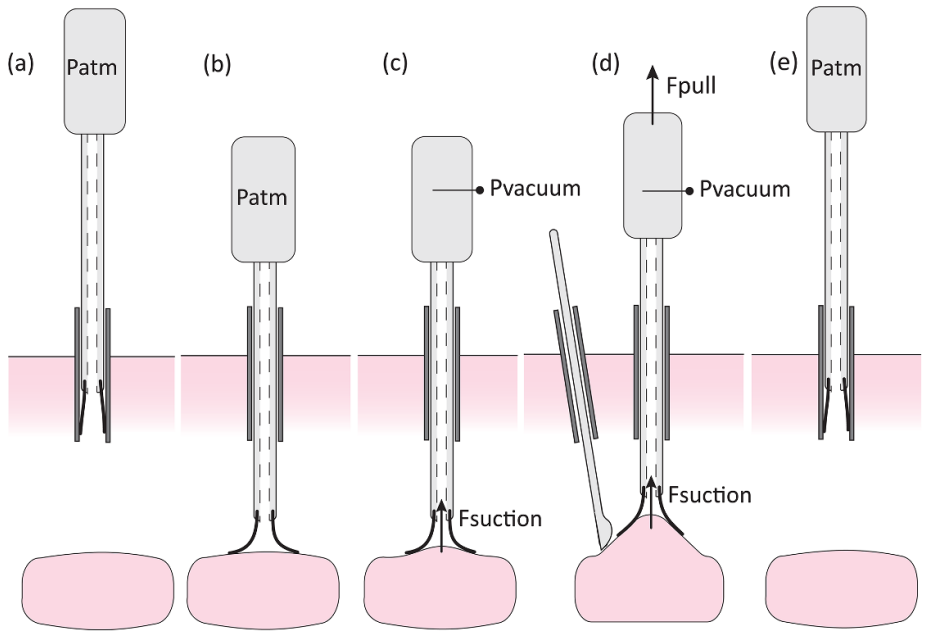

Figure 7. Schematic overview of the use scenario of the suction gripper. (a) The suction gripper is pushed through the trocar in the folded position. (b) The suction tip unfolds and makes contact with the target tissue to ensure a sufficient seal. (c) A vacuum pressure is generated to fixate the suction gripper to the target tissue. (d) The suction gripper provides stable support for tissue manipulations. (e) The target tissue detaches after the vacuum pressure is released. The gripper is pulled back through the trocar.

(figures 7(a) and (b)). A vacuum pressure is generated to fixate the suction gripper on the tissue surface (figure 7(c)). The tissue is pulled into the suction tip due to the applied vacuum pressure. The firm grip secures stable tissue lifting and stretching during tissue manipulations (figure 7(d)). At the end of the procedure, the vacuum pressure is released and the suction tip returns into its folded state when retracted into the trocar (figure 7(e)).

3.3. Fabrication suction tip

A prototype of the suction tip was built to validate its attachment performance. Dimensional stability and foldability of the suction tip were provided by flat nylon rays. The nylon rays were pre-bent into a semi circular shape by heating them while being pressed around a rod. A finely woven mesh was glued between the rays (universal contact glue, Bison). The air-tight film was fabricated using silicone (Smooth Sil, Smooth-on Inc. USA) with a shore hardness of 40A. This type of silicone has the perfect balance between flexibility, allowing the tip to fold and stiffness to maintain dimensional stability. For the deposition of a thin silicone layer on the mesh, a fabrication method inspired by gravity-based dip-coating was used (figure 8). First, the silicone mixture was poured into the suction tip, creating a silicone basin. Secondly, the suction tip was hung above a drainage platform. Gravitational forces drained the mixture from the silicone basin. During curing, the silicone mechanically interlocked with the mesh. The outer

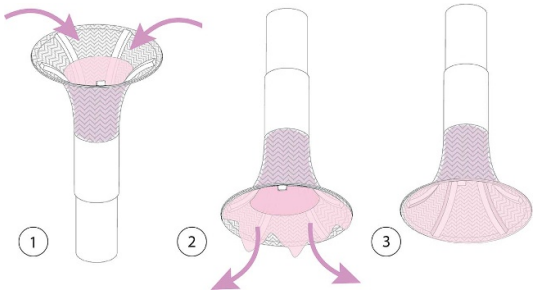

Figure 8. Procedure of gravity-based dip coating of the suction tip. A basin of uncured silicones is created inside the tip and gravity forces drain the mixture.

layer of the suction tip was fabricated by revolving a thin polyethylene foil around the suction tip.

Ecoflex 00-30 (Smooth-on Inc. USA) was used to fabricate the footprint. This silicone was chosen due to its high elongation rate of 900%, making it suitable to adapt to the shape of the tissue. In order to create the footprint, a thin film of uncured Ecoflex was smeared on a flat plate. The suction tip was placed on this uncured layer to attach the Ecoflex silicone air-tight to the Smooth Sil silicone while curing (figure 9).

The suction surface of the suction tip was made as large as possible, while still being able to slide in and out a ∅ 10 mm trocar (figure 10). This resulted in a suction surface with a 15 mm diameter in the unfolded state.

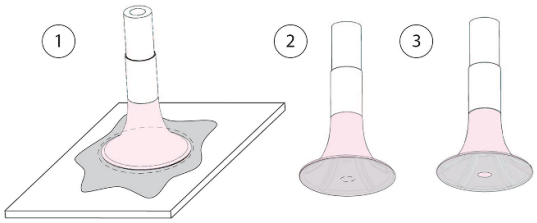

Figure 9. Fabrication process of the footprint layer. (1) A thin film of Ecoflex silicone is smeared on a plate. (2) After curing, the footprint is cut around the edge. (3) The closed footprint is cut open.

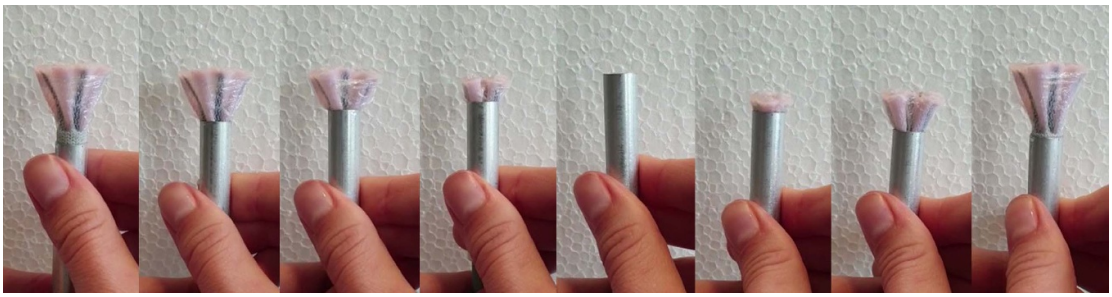

Figure 10. Video images of the final tip design extracted and retracted into a ∅ 10 mm tube with 0.5 mm wall thickness, representing the trocar.

4. Experimental validation

4.1. Experimental goal

The main goal of the experiments was to investigate the performance of the flexible suction tip, by (1) assessing the attachment performance of the suction tip on diverse (phantom) tissues and (2) measuring the effect of the vacuum pressure on the attachment performance.

4.2. Experimental setup

The experimental setup is illustrated in figures 11(a)–(d). In this experimental setup, the suction tip was connected to a 30 ml syringe by tubing with high buckling resistance (FESTO PAN-6x1). The suction tip was connected to an s-beam junior load cell (FUTEK, model FLLSB200) via a wire. This wire assured that the suction tip could move freely and, therefore, prevented premature detachment due to peel-off forces. Figure 11(a) shows a closeup of this part of the setup. The load cell, in turn, was connected to a linear stage via a 3D-printed base plate. The linear stage (ALMOTION LT50-TR-G8-200) was connected to a 3D-printed support that functioned as a containment unit for the gelatin tissue phantoms and animal tissues. The linear stage allowed for controlled motion of the load cell with the attached suction tip and thus for measuring the detachment force. Next to pull-off forces, this setup was able to measure slide-off forces exerted on the suction tip by connecting the load cell to the tip using a pulley system (figure 11(d)). The friction between the pulley and the wire was negligible. The slide-off forces were exerted in line with the contact surface of the suction tip, preventing the generation of a moment that would tilt the suction tip. The vacuum pressure was measured by a vacuum sensor (NXP, model MPX4115AP) that was connected to the tubing of the suction unit using a T-piece connector. Both the load cell and the vacuum sensor were connected to an analogue signal conditioner (CPJ RAIL, SCAIME) and a data acquisition unit set at a sampling rate of 20 Hz (NI USB-6008, National Instruments Corporation).

4.3. Experimental design

4.3.1. Experimental variables

The detachment force of the suction tip was the main performance measure of the suction tip. The detachment force was defined as the force required to detach the suction tip from its substrate and could either be orientated perpendicular (pull-off force) or parallel (slide-off force) to the contact surface. The detachment force was tested on a variety of substrates and vacuum pressures. Phantom tissues were manufactured to mimic tissues with varying stiffness, see table 2. A plexiglass plate was used as reference to compare the measurements of the phantom tissues with a fully stiff substrate. All phantoms and the plexiglass substrate were tested in dry and lubricated conditions, as it was expected that the mucus layer of tissues might influence the performance of the suction tip. Vacuum pressures of 30 kPa, 40 kPa, 50 kPa, 60 kPa and 70 kPa were used. Additionally, experiments were conducted at the Skillslab in Erasmus

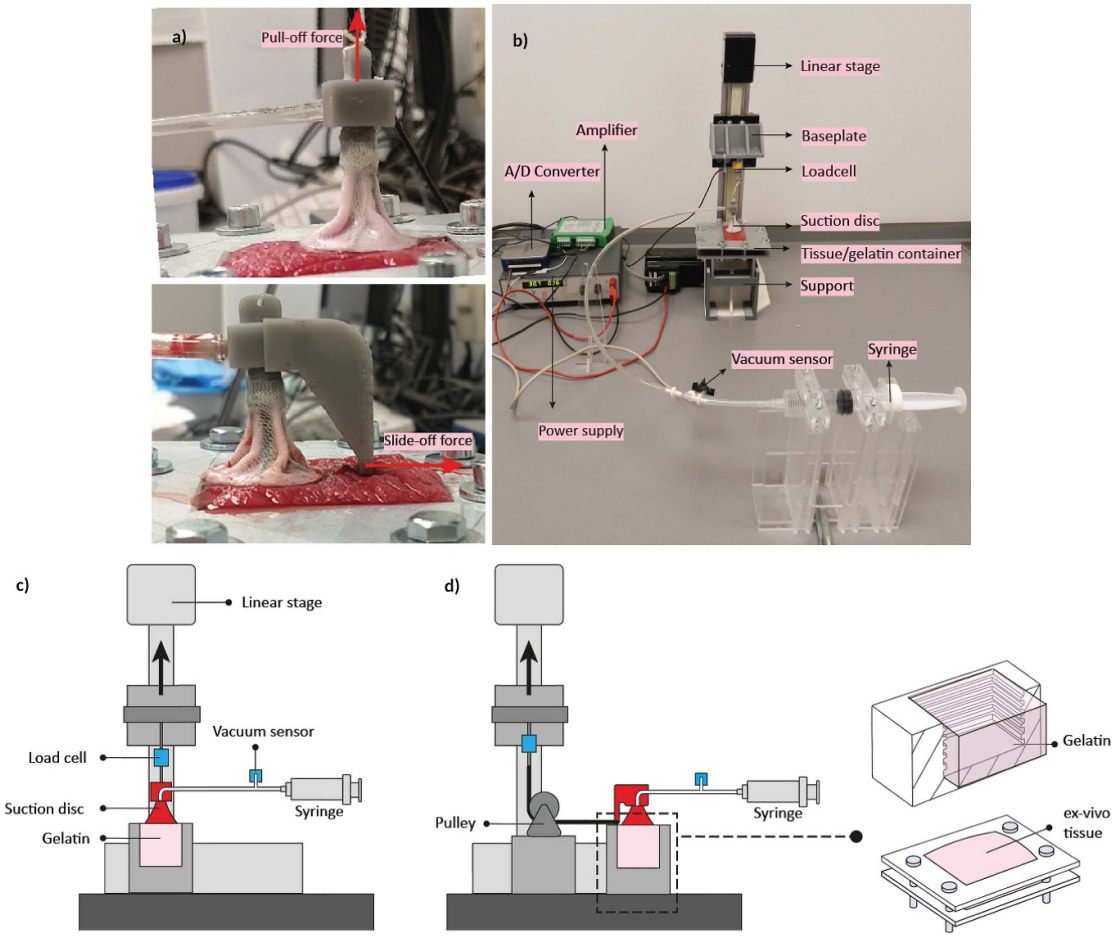

Figure 11. Experimental facility. (a) The suction tip connected to the linear stage and the syringe, for pull-off measurements and slide-off measurements. (b) Overview of the experimental setup to measure the detachment forces. (c) Schematic overview of the experimental setup generating pull-off forces. (d) Schematic overview of the experimental setup generating slide-off forces.

Table 2. Phantom tissues are made with three different gelatin ratios to mimic three tissues with varying stiffness.

Phantom tissue	Gelatin percentage (wt%)	Stiffness (kPa)	Source
Skeletal muscle tissue	15	31	[59, 60]
Liver tissue	10	17	[60, 61]
Brain tissue	5	5.3	[60, 62]

Medical Centre (Rotterdam, the Netherlands) using *ex vivo* chicken liver tissue and *ex vivo* cow muscle tissue.

4.3.2. Experimental protocol

At the start of each experiment, the load cell was calibrated by subtracting the weight of the suction tip from the measured pull-off force. Next, the suction tip was placed on the substrate and the vacuum pressure was generated by pulling the syringe manually. The syringe was pulled until the desired vacuum pressure was reached, which was monitored in LabVIEW. 3D-printed clamps fixated the syringe at the desired position. The linear stage moved upward with a velocity of $1\,\mathrm{mm\,s^{-1}}$. In order to achieve constant starting conditions, the following two steps were taken. First, the suction tip was placed on the substrate with an untensioned wire. This ensures that no initial traction was applied to the load cell at the moment of vacuum initiation. Secondly, the tubing connected to the suction base was supported, as its weight could otherwise tilt the suction tip and break the seal. The gelatin was poured into containers with horizontal grooves on the inside to prevent the gelatin from getting lifted during the experiment. As gelatin degrades over time, only gelatin made the same day was used for experiments. The animal tissue samples were fixated between two surfaces of a 3D-printed clamp.

The main experiment was subdivided into two sub-experiments: (1) Experiment 1: Effect of the substrate and (2) Experiment 2: Effect of vacuum pressure. In Experiment 1, the suction tip was tested on different gelatin tissue phantoms, the plexiglass reference substrate and the *ex vivo* tissue samples.

Experiment 1 was further subdivided into five sub-experiments:

- Experiment 1.1. Pull-off measurements on lubricated phantom tissues.
- Experiment 1.2. Pull-off measurements on dry phantom tissues.
- Experiment 1.3. Pull-off measurements on *ex vivo* tissue samples.
- Experiment 1.4. Slide-off measurements on lubricated phantom tissues.
- Experiment 1.5. Slide-off measurements on *ex vivo* tissue samples.

The vacuum pressure was set to 50 kPa for all measurements of Experiment 1, based on the vacuum pressure of the commercially used *Octopus heart stabilizer* (Medtronic). The phantom tissues were lubricated with a thin layer of water-based lubricant. The slide-off measurements were performed on lubricated phantom tissues as these generally reassemble the surface properties of tissues closest, being surrounded by a slippery mucus layer. Measurements of Experiment 2 were all performed on lubricated phantom tissue made of 10 wt% gelatin while being subjected to pull-off forces. Vacuum pressures were generated in a range of 30 kPa–70 kPa. Five trials per condition were executed for all experiments.

- Experiment 2. Pull-off measurements using vacuum pressures in a range of 30 kPa–70 kPa.

4.3.3. Data analysis

The data of the pressure sensor and load cell was obtained using Labview 2013. From this data, the average detachment force ± standard deviation was calculated. The data from Experiment 1.1 was analyzed by a one-way ANOVA test to examine if the attachment performance when being subjected to pull-off forces is significantly different for the different substrates. Also, the average detachment force onto lubricated substrates obtained in Experiment 1.1 was compared with the average detachment force onto dry substrates obtained in Experiment 1.2 by an independent two-sided t-test. The data from Experiment 1.3 was analyzed using an independent two-sided t-test to examine if the attachment performance when being subjected to pull-off forces is significantly different for the muscle and liver tissue samples. Furthermore, the data from Experiment 2 was analyzed by a one-way ANOVA test in order to identify if the attachment performance is significantly different for the different vacuum pressures. The statistical significance was set at an α value of less than 0.05. The linearity of the relationship between vacuum pressure and detachment force was analyzed by the correlation coefficient.

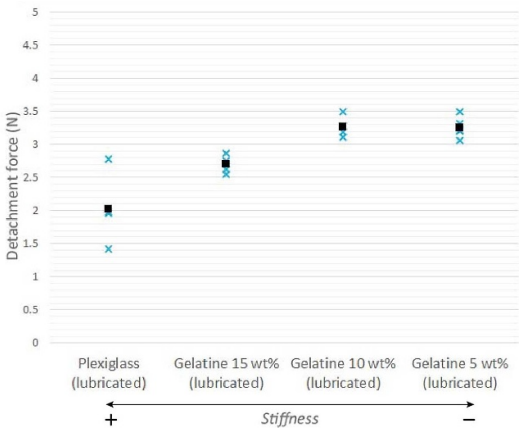

Figure 12. Attachment performance against pull-off forces of the suction tip for lubricated substrates that differ in stiffness. The black square represents the average detachment force and the blue crosses represent the individual measurements.

5. Results

5.1. Pull-off measurements

5.1.1. Experiment 1.1: lubricated phantom tissue

Experiment 1.1 showed that the suction tip induced higher detachment forces to the substrates with a lower stiffness, as illustrated in figure 12. The average detachment force against pull-off forces and its standard deviation on the lubricated plexiglass plate, lubricated 15 wt% gelatin, lubricated 10 wt% gelatin and lubricated 5 wt% gelatin were 2.02 ± 0.49 N, 2.7 ± 0.13 N, 3.27 ± 0.15 N and 3.26 ± 0.16 N, respectively. A one-way ANOVA test shows that the difference between performance outcomes of the substrates is significant ($F(3,16) = 23.35$, $p = 4.4 \times 10^{-6}$). It was noticeable that the suction tip failed a few times in its initial attachment on the plexiglass plate, while this did not happen with the gelatin phantom tissues. Furthermore, the observation was made that detachment from the rigid substrates (the plexiglass plate and 15 wt% gelatin) was often due to a V-shaped indentation (see figure 13), while the perimeter of the suction tip kept its circular shape during detachment from the flexible substrates.

5.1.2. Experiment 1.2: dry phantom tissue

The attachment performance of the suction tip against pull-off forces on dry substrates is illustrated in figure 14. The average detachment force and its standard deviation on the dry plexiglass plate, dry 15 wt% gelatin, dry 10 wt% gelatin and dry 5 wt% gelatin were 2.04 ± 0.12 N, 3.79 ± 0.41 N, 4.03 ± 0.28 N and 3.68 ± 0.33 N, respectively. One-way ANOVA testing shows that the difference in performance outcomes between the substrates is significant ($F(3,16) = 17.51$, $p = 2.6 \times 10^{-5}$). An independent t-test shows an insignificant effect on

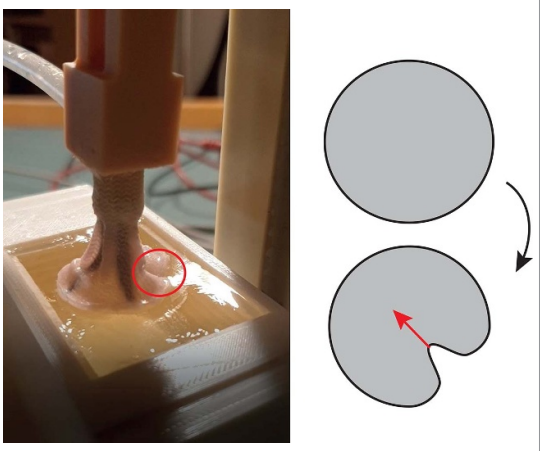

Figure 13. Detachment of the suction tip. At the left, a video image of the moment before detachment is shown for a 15 wt% gelatin substrate. The red circle encircles the inward slip of the rim, which causes detachment. At the right, this inward slip is schematically visualized from above.

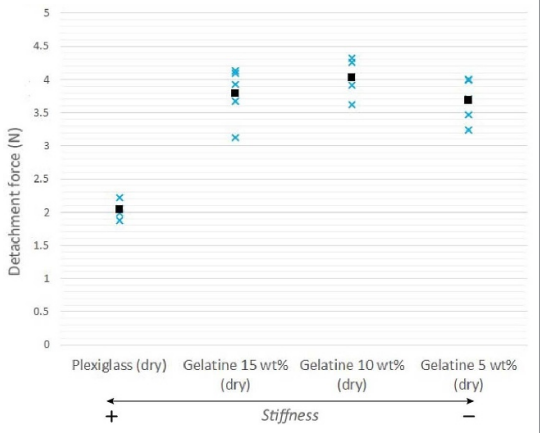

Figure 14. Attachment performance of the suction tip against pull-off forces for dry substrates that differ in stiffness. The black square represents the average detachment force and the blue crosses represent the individual measurements.

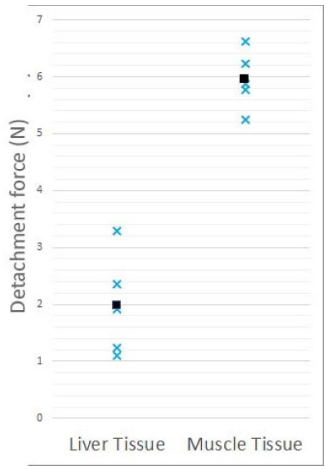

Figure 15. Attachment performance against pull-off forces of the suction tip for on *ex vivo* liver tissue and *ex vivo* muscle tissue. The black square represents the average detachment force and the blue crosses represent the individual measurements.

the detachment force on the rigid plexiglass plate ($t(8) = 0.0816$, $p = 0.9369$) between the dry and lubricated state. However, there is a significant effect on the detachment force on the 15 wt% gelatin ($t(8) = 5.6733$, $p = 4.6861 \times 10^{-04}$), the 10 wt% gelatin ($t(8) = 5.3835$, $p = 6.5885 \times 10^{-04}$) and the 5 wt% gelatin ($t(8) = 2.4758$, $p = 0.0384$) between dry and lubricated states. Overall, the suction tip performs better on dry tissue compared to lubricated tissue.

5.1.3. Experiment 1.3: ex vivo *tissue samples*

The attachment performance of the suction tip against pull-off forces on *ex vivo* animal tissue samples is illustrated in figure 15. The average detachment force and its standard deviation on the liver tissue sample and the muscle tissue sample are 1.98 ± 0.90 N and 5.95 ± 0.52 N, respectively. An independent t-test shows that the difference in performance outcomes between the tissues is significant ($t(8) = 8.5783$, $p = 2.6333 \times 10^{-05}$). The suction tip performed less well on the liver tissue sample compared to the liver's phantom counterpart, whereas it performed better on the muscle tissue sample compared to the muscle's phantom counterpart.

5.2. Slide-off measurements

5.2.1. Experiment 1.4: lubricated phantom tissues

The average detachment force against slide-off forces and its standard deviation on the lubricated plexiglass plate was 4.61 ± 0.96 N. The suction tip was observed to slide over the plexiglass plate's surface before it detached at once. No detachment force could be measured for the lubricated 15 wt% gelatin and the lubricated 10 wt% gelatin, as the suction tip kept sliding over the gelatin phantoms without detaching. The average attachment force before the suction tip started sliding for the 15 wt% and 10 wt% gelatin phantoms were 2.06 ± 0.35 N and 1.38 ± 0.20 N, respectively. The suction tip did stop sliding on the lubricated 5 wt% gelatin. However, the gelatin broke before the detachment force could be reached. The reached average attachment force before the 5 wt% gelatin broke was 1.99 ± 0.35 N.

5.2.2. Experiment 1.5: ex vivo *tissue samples*

The slide-off measurements on the *ex vivo* animal tissue samples showed that the suction tip did not find grip on both surfaces. The suction tip kept sliding over the liver tissue until the end of the sample was reached, or until the tissue slipped out of the suction tip during sliding. The average attachment force during sliding was 1.74 ± 0.8 N. The suction tip kept sliding over the muscle tissue sample until it touched a bump in the tissue surface. The average detachment force of the suction tip on muscle tissue was 6.37 ± 0.41 N.

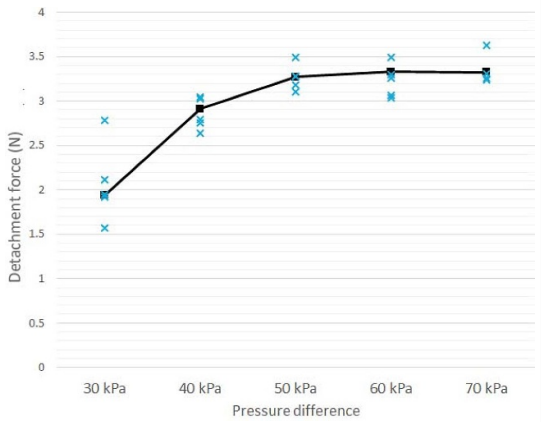

Figure 16. Attachment performance against pull-off forces for different vacuum pressure differences on 10 wt% gelatin. The black square represents the average detachment force and the blue crosses represent the individual measurements.

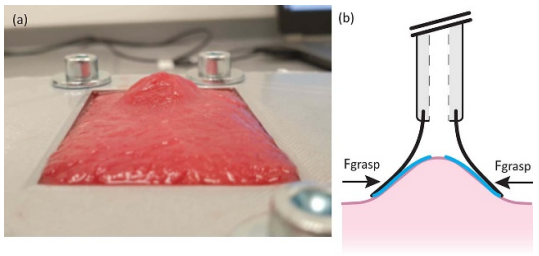

Figure 17. (a) Imprint of the suction tip on the *ex vivo* muscle tissue sample. (b) Tissue is pulled into the suction tip, resulting in additional grasping forces (F_{grasp}) and an expansion of the suction surface.

5.3. Experiment 2: vacuum pressure

Experiment 2 showed that the relationship between the detachment force and the vacuum pressure is non-linear (figure 16). The relationship between the detachment force and vacuum pressure flattens out for higher vacuum pressures. The correlation coefficient r of the relationship is 0.85. The mean detachment force and its standard deviation with a vacuum pressure of 30 kPa, 40 kPa, 50 kPa, 60 kPa and 70 kPa were 1.94 ± 0.23 N, 2.91 ± 0.19 N, 3.27 ± 0.15 N, 3.33 ± 0.21 N and 3.32 ± 0.18 N, respectively. One-way ANOVA testing shows that the difference in performance outcomes between the pressures is significant at $p < 0.05$ ($F(4, 20) = 47.62$, $p = 6 \times 10^{-10}$). An independent t-test shows no significant difference in the detachment force with a vacuum pressure of 60 kPa and 70 kPa ($t(8) = 1.0047, p = 0.3445$).

6. Discussion

6.1. Main findings

In this study, we have developed the first bio-inspired suction disc design for a suction gripper in MIS. A proof-of-principle experiment showed that the developed suction tip was able to successfully and safely grip slippery tissues without enclosing them.

Noticeably, the attachment performance of the suction tip was higher on flexible substrates than on rigid substrates. The muscle tissue sample showed clear imprints of the suction tip after a measurement, which reveals that the suction tip is performing a shape grip onto the flexible tissue surface (figure 17(a)). The tissue is pulled into the suction tip, where the tip's perimeter grasps the flexible tissue, somewhat similar to how a conventional gripper grips tissues (figure 17(b)). This results in improved sealing and additional grip when attached to flexible substrates. Also, pulling the tissue into the suction tip results in an expansion of the suction surface, as more tissue surface is directly affected by the vacuum pressure. Figure 18 shows the force-time graphs and vacuum pressure-time graphs of a trial with the lubricated plexiglass plate and a typical trial with lubricated 10 wt% gelatin, subjected to pull-off forces. It shows that more leakage occurs during the attachment onto the rigid plexiglass plate, whereas less vacuum pressure is lost during attachment on the flexible gelatin. This substantiates that the suction tip seals better on flexible substrates.

When subjected to shear forces, the suction tip's shape grip again enhanced its attachment performance. The highly flexible 5 wt% gelatin was deformed sufficiently into the suction tip to prevent the tip from sliding over the slippery surface. The shape grip was insufficient on the 10 wt% gelatin, the 15 wt% gelatin and the plexiglass plate to prevent the suction tip from sliding. In future research, we propose to look into strategies that increase the grip of the footprint layer to lower the risk of sliding. Nature shows that this could be done by adding a microstructure on the footprint's surface [24, 31]. Optionally, the vacuum pressure could be increased when slip is detected, either by eye or an integrated sensing system.

Furthermore, it was observed that the suction tip had more grip on the dry substrates than on the lubricated substrates. This could be caused by the higher friction coefficient between the footprint and the dry substrate, which counteracts inward slip of the rim and thereby results in delayed detachment. This would explain why detachment forces of the suction tip are higher on the muscle tissue sample than the liver tissue sample for both the pull-off measurements and the shear measurements. Although the liver tissue is more flexible than the muscle tissue, its surface is covered by a highly slippery mucus layer. Overall, these results show that the suction tip performs best on flexible and dry tissues.

Increasing the vacuum pressure from 30 kPa to 70 kPa showed a relationship with the attachment force that acted linearly for low vacuum pressures, and flattens out for high vacuum pressures. It could

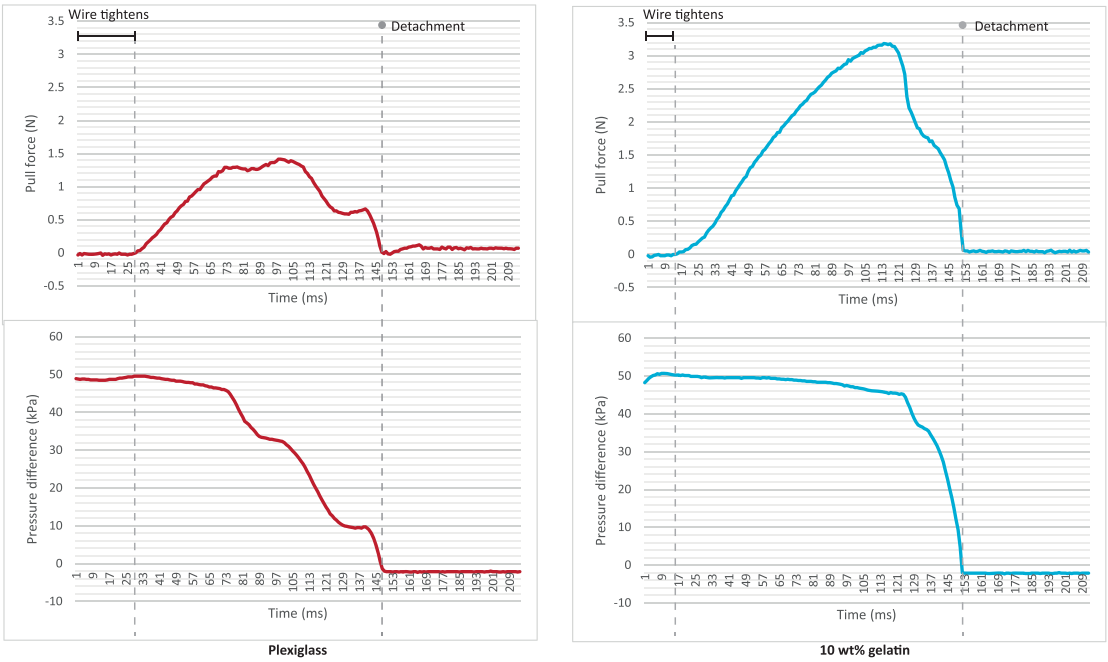

Figure 18. Occurrence of leakage during measurements when subjected to pull-off forces. Left: force-time and pressure-time graphs of a measurement with the lubricated plexiglass plate as substrate. Right: force-time and vacuum pressure-time graphs of a measurement with lubricated 10 wt% gelatin as substrate. More leakage before detachment occurs with the rigid substrate compared to the flexible substrate, which means the suction tip seals better with flexible substrates. Both measurements were performed with an initial pressure difference of 50 kPa.

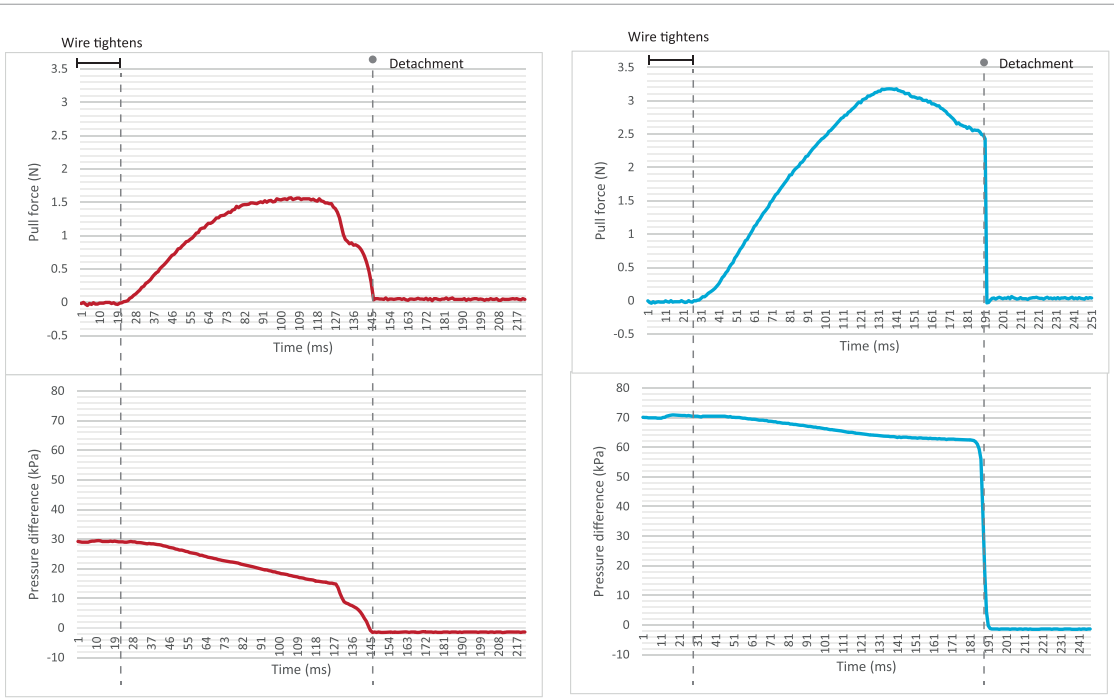

Figure 19. Occurrence of leakage during measurements when being subjected to pull-off forces. Left: force-time and vacuum pressure-time graphs of a measurement with an initial pressure difference of 30 kPa. Right: force-time and vacuum pressure-time graphs of a measurement with an initial pressure of 70 kPa. More leakage before detachment occurs using a low initial pressure difference compared to a high initial pressure difference. Both measurements were performed with a lubricated 10 wt% substrate.

be hypothesized that the substrate is pulled more into the suction tip using high vacuum pressures, increasing the foot print surface and thus the resistance to leakage. At some point, the substrate is maximally deformed and no longer affected by higher vacuum pressures. This would explain why the curve in figure 16 flattens out for higher vacuum pressures. The force-time graphs of a typical measurement (figure 19) indeed show more leakage during attachment at lower actuation pressures.

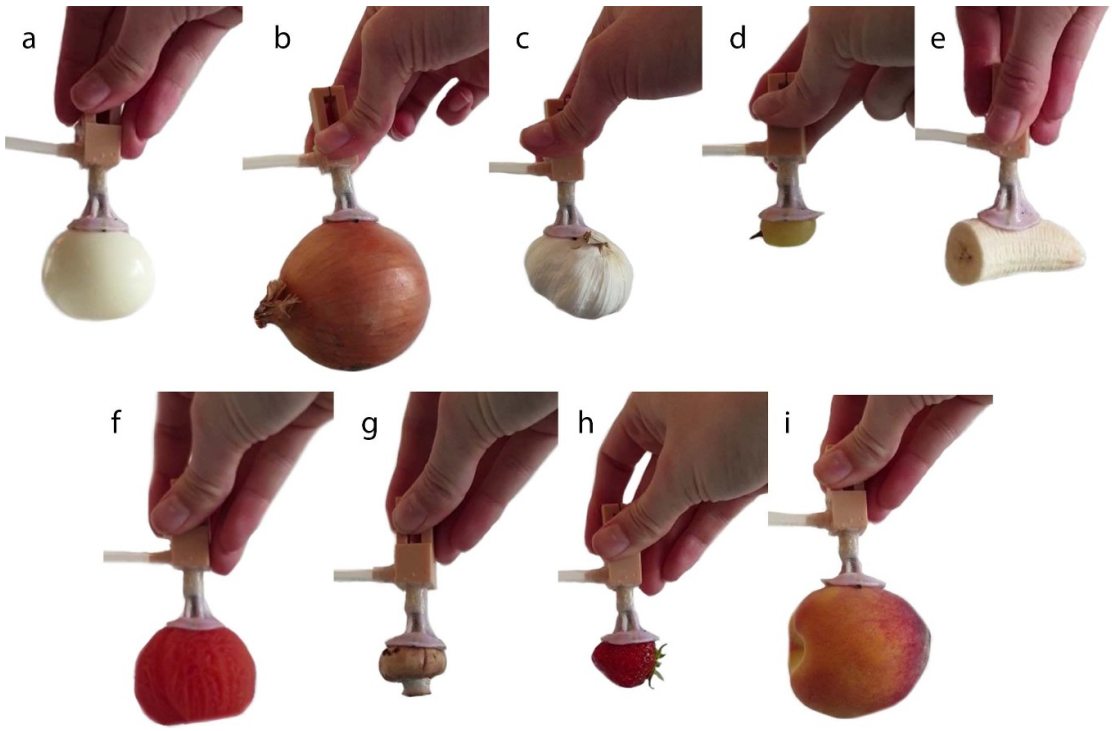

Figure 20. Demonstration of gripping objects with varying substrate characteristics, namely; (a) peeled egg, (b) onion, (c) garlic, (d) grape, (e) banana, (f) peeled tomato, (g) cooked mushroom, (h) strawberry and (i) peach.

The developed suction tip was able to exert a maximal detachment force of 3.27 ± 0.15 N on slippery, flexible phantom tissue, 1.98 ± 0.90 N on liver tissue and 5.95 ± 0.524 N on muscle tissue. Theoretically, all listed organs in table 1 can be lifted by these attachment forces. It could be argued that heavy organs would be lifted by multiple suction grippers anyway, to prevent local stress accumulation. Figure 20 shows the suction tip's ability to lift some arbitrary objects with varying shapes and surface characteristics. The tip is able to grip objects smaller than the suction tip's perimeter by adapting its shape to the object. Figure 21 shows how the suction tip is able to lift a slippery chicken heart. During surgery, the vacuum pressure should be monitored and optimized in order to gain sufficient grip on different tissue types, or multiple smaller suction gripper could be used to ensure proper attachment.

6.2. Application fields

In some specific applications, it could be favorable to use a suction gripper over a conventional gripper. For example, literature mentions the merit of using suction gripping in bowel and colon manipulations, as these thin membranes are most delicate and easily damaged by squeezing forces of the gripper's jaws [13, 18]. Another application for the suction gripper would be the fixation of voluminous slippery tissue, e.g. liver tissue, during the execution of a biopsy.

6.3. Limitations

This study is subjected to some limitations. The exploratory nature of this study provides only initial insights into the performance behavior of the suction gripper. Future research, including *in vivo* studies, should show in which procedures the use of our suction gripper is favorable over a conventional gripper.

6.4. Design recommendations

For the device, some development steps are recommended to increase its potential. First, more research should be focused on optimizing the vacuum actuation, either manually or by a vacuum pump. Figure 22 shows a first prototype in which a vacuum chamber is integrated into the suction gripper's handle to facilitate manual actuation. Furthermore, future research should optimize the properties of the footprint layer in terms of grip and flexibility. Future studies should focus on *in vivo* experiments to evaluate the performance of the suction gripper in a realistic clinical setting. Biocompatible alternatives should be found for the materials that are currently incorporated in the prototype, before testing on porcine models. Miniaturization of the suction gripper, striving for an outer diameter of 5 mm, is required to function as an equal alternative to the conventional gripper in minimally invasive procedures. Optimization of the folding mechanism could result

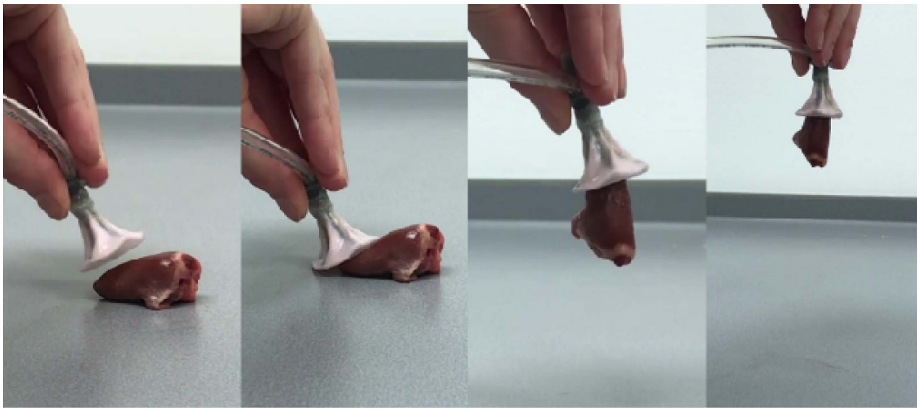

Figure 21. Demonstration of the suction tip lifting a chicken heart, where the tip's shape grip enhances its sealing.

Figure 22. Vacuum handle (adapted from a *Kiwi* vacuum assisted delivery system) integrated with the bio-inspired suction tip.

in a higher gain in the vacuum surface when converting from a folded into an unfolded state. Here, the nylon rays of the current folding mechanism could be replaced by superelastic nitinol wires. These nitinol wires have as an additional advantage that they can be accurately shaped using heat, which increases the shape consistency and durability of the suction grippers. These design recommendations will contribute to increasing the potential of our suction-based tissue gripper.

7. Conclusion

This study presented the development and successful first validation of a bio-inspired suction gripper for MIS. Similar to biological suction discs, our developed gripper is divided into two main parts: (1) the suction chamber inside the handle in which vacuum pressure is generated and (2) the suction tip that attaches to the target tissue and allows for tissue manipulation during MIS. The suction tip consists of five layers to allow the suction tip to expand into a bigger surface area (foldability), to create an air-tight tip (air-tightness), to allow for a smooth transition of the suction tip through the trocar (slideability) and to create an air-tight seal with the tissue (seal generation) while magnifying frictional support (friction magnification). The experiments illustrated that our suction gripper outperforms man-made suction discs, as well as currently described suction grippers in literature in terms of attachment force (5.61 versus 5.95 N [18]) and substrate versatility (figures 20 and 21). The suction tip's shape grip enhances its resistance against slipping during the shear experiments and adapts the tip's shape to grip objects smaller than the suction tip's outer diameter. Our bio-inspired suction gripper offers the opportunity for a safer alternative to the conventional tissue gripper in MIS.

Data availability statement

The data that support the findings of this study are available upon reasonable request from the authors.

Acknowledgment

We would like to thank Manja Muijtjens for facilitating the experiments in the Skillslab of the Erasmus Medical Centre.

ORCID iDs

Vera G Kortman https://orcid.org/0000-0002-2370-0013
Aimée Sakes https://orcid.org/0000-0002-4323-884X

References

[1] de Visser H, Heijnsdijk E A M, Herder J L and Pistecky P V 2002 Forces and displacements in colon surgery *Surg. Endosc.* **16** 14263–1430
[2] Wang J, Ma L, Li W and Zhou Z 2018 Safety of laparoscopic graspers with different configurations during liver tissue clamping *Biosurf. Biotribol.* **4** 50–57
[3] Cartmill J A, Shakeshaft A J, Walsh W R and Martin C J 1999 High pressures are generated at the tip of laparoscopic graspers *ANZ J. Surg.* **69** 127–30
[4] Marucci D D, Cartmill J A, Walsh W R and Martin C J 2000 Patterns of failure at the instrument–tissue interface *J. Surg. Res.* **93** 16–20
[5] Heijnsdijk E A M, Dankelman J and Gouma D J 2002 Effectiveness of grasping and duration of clamping using laparoscopic graspers *Surg. Endosc.* **16** 1329–31
[6] Van der Voort M, Heijnsdijk E A M and Gouma D J 2004 Bowel injury as a complication of laparoscopy *J. Br. Surg.* **91** 1253–8
[7] Joice P, Hanna G B and Cuschieri A 1998 Errors enacted during endoscopic surgery—a human reliability analysis *Appl. Ergon.* **29** 409–14
[8] Khan A F, MacDonald M K, Streutker C, Rowsell C, Drake J and Grantcharov T 2021 Tissue stress from laparoscopic grasper use and bowel injury in humans: establishing intraoperative force boundaries *BMJ Surg., Interventions Health Technol.* **3** e000084
[9] Scott N A, Knight J L, Bidstrup B P, Wolfenden H, Linacre R N and Maddern G J 2002 Systematic review of beating heart surgery with the octopus tissue stabilizer *Eur. J. Cardio-Thorac. Surg.* **21** 804–17
[10] Singh S K, Tewarson V, Gupta S and Kumar S 2013 Making octopus tissue stabilizer more effective—a valuable technique *Indian J. Thorac. Cardiovasc. Surg.* **29** 52–54
[11] Jansen E W L, Lahpor J R, Borst C, Gründeman P F and Bredée J J 1998 Off-pump coronary bypass grafting: how to use the octopus tissue stabilizer *Ann. Thorac. Surg.* **66** 576–9
[12] Jansen E W L, Borst C, Lahpor J R, Gründeman P F, Eefting F D, Nierich A, de Medina E O R and Bredée J J 1998 Coronary artery bypass grafting without cardiopulmonary bypass using the octopus method: results in the first one hundred patients *J. Thorac. Cardiovasc. Surg.* **116** 60–67
[13] Ranzani T, Russo S, Walsh C and Wood R 2016 A soft suction based end effector for endoluminal tissue manipulation *in vitro* **1** 1–5
[14] Becker S, Ranzani T, Russo S and Wood R J 2017 Pop-up tissue retraction mechanism for endoscopic surgery *2017 IEEE/RSJ Int. Conf. on Intelligent Robots and Systems (IROS)* (IEEE) pp 920–7
[15] Horie T, Sawano S and Konishi S 2007 Micro switchable sucker for fixable and mobile mechanism of medical MEMS *2007 IEEE 20th Int. Conf. on Micro Electro Mechanical Systems (MEMS)* (IEEE) pp 691–4
[16] Patronik N A, Zenati M A and Riviere C N 2005 Preliminary evaluation of a mobile robotic device for navigation and intervention on the beating heart *Comput. Aided Surg.* **10** 225–32
[17] Patronik N A, Ota T, Zenati M A and Riviere C N 2009 A miniature mobile robot for navigation and positioning on the beating heart *IEEE Trans. Robot.* **25** 1109–24
[18] Vonck D, Jakimowicz J J, Lopuhaä H P and Goossens R H M 2012 Grasping soft tissue by means of vacuum technique *Med. Eng. Phys.* **34** 1088–94
[19] Osaki M, Omata T, Takayama T and Ohizumi H 2011 Transformable lung positioner for thoracoscopic surgery *2011 IEEE/SICE Int. Symp. on System Integration (SII)* (IEEE) pp 138–43
[20] Kier W M and Smith A M 2002 The structure and adhesive mechanism of octopus suckers *Integr. Comp. Biol.* **42** 1146–53
[21] Ditsche P and Summers A 2019 Learning from northern clingfish (*Gobiesox maeandricus*): bioinspired suction cups attach to rough surfaces *Phil. Trans. R. Soc.* B **374** 20190204
[22] Tramacere F, Beccai L, Mattioli F, Sinibaldi E and Mazzolai B 2012 Artificial adhesion mechanisms inspired by octopus suckers *2012 IEEE Int. Conf. on Robotics and Automation* (IEEE) pp 3846–51
[23] Wainwright D K, Kleinteich T, Kleinteich A, Gorb S N and Summers A P 2013 Stick tight: suction adhesion on irregular surfaces in the northern clingfish *Biol. Lett.* **9** 20130234
[24] Ditsche P, Wainwright D K and Summers A P 2014 Attachment to challenging substrates–fouling, roughness and limits of adhesion in the northern clingfish (*Gobiesox maeandricus*) *J. Exp. Biol.* **217** 2548–54
[25] Kang V, White R T, Chen S and Federle W 2021 Extreme suction attachment performance from specialised insects living in mountain streams (Diptera: Blephariceridae) *Elife* **10** e63250
[26] Tramacere F, Appel E, Mazzolai B and Gorb S N 2014 Hairy suckers: the surface microstructure and its possible functional significance in the *Octopus vulgaris* sucker *Beilstein J. Nanotechnol.* **5** 561–5
[27] Smith J E 1947 The activities of the tube feet of *Asterias Rubens* L: I. The mechanics of movement and of posture *J. Cell Sci.* **3** 1–14
[28] Nichols D 1959 The histology and activities of the tube-feet of *Echinocyamus pusillus J. Cell Sci.* **3** 539–55
[29] Maie T, Schoenfuss H L and Blob R W 2013 Musculoskeletal determinants of pelvic sucker function in Hawaiian stream gobiid fishes: interspecific comparisons and allometric scaling *J. Morphol.* **274** 733–42
[30] De Meyer J and Geerinckx T 2014 Using the whole body as a sucker: combining respiration and feeding with an attached lifestyle in hill stream loaches (Balitoridae, Cypriniformes) *J. Morphol.* **275** 1066–79
[31] Chuang Y, Chang H, Liu G and Chen P 2017 Climbing upstream: multi-scale structural characterization and underwater adhesion of the Pulin river loach (*Sinogastromyzon puliensis*) *J. Mech. Behav. Biomed. Mater.* **73** 76–85
[32] Tramacere F, Follador M, Pugno N M and Mazzolai B 2015 Octopus-like suction cups: from natural to artificial solutions *Bioinspir. Biomim.* **10** 035004
[33] Sandoval J A, Jadhav S, Quan H, Deheyn D D and Tolley M T 2019 Reversible adhesion to rough surfaces both in and out of water, inspired by the clingfish suction disc *Bioinspir. Biomim.* **14** 066016
[34] Sadeghi A, Beccai L and Mazzolai B 2012 Design and development of innovative adhesive suckers inspired by the tube feet of sea urchins *2012 4th IEEE RAS and EMBS Int. Conf. on Biomedical Robotics and Biomechatronics (BioRob)* (IEEE) pp 617–22
[35] Tramacere F, Pugno N M, Kuba M J and Mazzolai B 2015 Unveiling the morphology of the acetabulum in *Octopus suckers* and its role in attachment *Interface Focus* **5** 20140050
[36] Tramacere F, Kovalev A, Kleinteich T, Gorb S N and Mazzolai B 2014 Structure and mechanical properties of *Octopus vulgaris* suckers *J. R. Soc. Interface* **11** 20130816

[37] Tramacere F, Beccai L, Kuba M, Gozzi A B and Mazzolai B 2013 The morphology and adhesion mechanism of *Octopus vulgaris* suckers *PLoS One* **8** e65074
[38] Max Z 1936 Suction cup *US Patent* 2055397
[39] Tiwari A and Persson B N J 2019 Physics of suction cups *Soft Matter* **15** 9482–99
[40] Green D M and Barber D L 1988 The ventral adhesive disc of the clingfish *Gobiesox maeandricus*: integumental structure and adhesive mechanisms *Can. J. Zool.* **66** 1610–9
[41] Arita G S 1967 A comparative study of the structure and function of the adhesive apparatus of the cyclopteridae and gobiesocidae *Master's Thesis* University of British Columbia (https://doi.org/10.14288/1.0104391)
[42] Beckert M, Flammang B E and Nadler J H 2016 A model of interfacial permeability for soft seals in marine-organism, suction-based adhesion *MRS Adv.* **1** 2531–43
[43] Persson B N J 2003 On the mechanism of adhesion in biological systems *J. Chem. Phys.* **118** 7614–21
[44] Persson B N J and Gorb S 2003 The effect of surface roughness on the adhesion of elastic plates with application to biological systems *J. Chem. Phys.* **119** 11437–44
[45] Bouaziz R, Truffault L, Borisov R, Ovalle C, Laiarinandrasana L, Miquelard-Garnier G and Fayolle B 2020 Elastic properties of polychloroprene rubbers in tension and compression during ageing *Polymers* **12** 2354
[46] Kier W M and Smith A M 1990 The morphology and mechanics of octopus suckers *Biol. Bull.* **178** 126–36
[47] Fulcher B A and Motta P J 2006 Suction disk performance of echeneid fishes *Can. J. Zool.* **84** 42–50
[48] Beckert M, Flammang B E and Nadler J H 2015 Remora fish suction pad attachment is enhanced by spinule friction *J. Exp. Biol.* **218** 3551–8
[49] Bhatia B 1950 Adaptive modifications in a hill-stream catfish, Glyptothorax telchitta (Hamilton) *Proc. Indian Natl Sci. Acad.* **16** 271–85
[50] Singh N and Agarwal N 1991 The SEM surface structure of the adhesive organ of *Pseudoechneis sulcatus* McClelland (Teleosti: sisoridae) from Garhwal Himalayan Hillstream *Acta Ichthyol. Piscat.* **XXI** 29–35
[51] Sinha A K, Singh T and Singh B R 1990 The morphology of the adhesive organ of the sisorid fish, Glyptothorax pectinopterus *Japan. J. Ichthyol.* **36** 427–31
[52] Conway K W, Lujan N K, Lundberg J G, Mayden R L and Siegel D S 2012 Microanatomy of the paired-fin pads of ostariophysan fishes (Teleostei: Ostariophysi) *J. Morphol.* **273** 1127–49
[53] Kang V, Johnston R, van de Kamp T, Faragó T and Federle W 2019 Morphology of powerful suction organs from blepharicerid larvae living in raging torrents *BMC Zool.* **4** 1–14
[54] Ingram A L and Parker A R 2005 The anatomy and attachment mechanism of the haptor of a *Capsala* sp.(Platyhelminthes: Monogenea: Capsalidae) on the blue marlin, *Makaira nigricans* (Istiophoridae) *J. Nat. Hist.* **39** 3633–47
[55] Borst C, Jansen E W L, Tulleken C A F, Grundeman P F, Beck H J M, van Dongen J W F, Hodde K C and Bredée J J 1996 Coronary artery bypass grafting without cardiopulmonary bypass and without interruption of native coronary flow using a novel anastomosis site restraining device ("Octopus") *J. Am. Coll. Cardiol.* **27** 1356–64
[56] Sheikhazadi A, Sadr S S, Ghadyani M H, Taheri S K, Manouchehri A A, Nazparvar B, Mehrpour O and Ghorbani M 2010 Study of the normal internal organ weights in Tehran's population *J. Forensic Leg. Med.* **17** 78–83
[57] de la Grandmaison G L, Clairand I and Durigon M 2001 Organ weight in 684 adult autopsies: new tables for a caucasoid population *Forensic Sci. Int.* **119** 149–54
[58] Dalbir Singh Y S B, Sreenivas M, Naresh Pandey A and Tyagi S 2004 Weights of human organs at autopsy in Chandigarh zone of north-west India *JIAFM* **26** 97–99
[59] Kot B C W, Zhang Z J, Lee A W C, Leung V Y F, Fu S N and Kellermayer M S 2012 Elastic modulus of muscle and tendon with shear wave ultrasound elastography: variations with different technical settings *PLoS One* **7** e44348
[60] Scali M, Breedveld P and Dodou D 2019 Experimental evaluation of a self-propelling bio-inspired needle in single-and multi-layered phantoms *Sci. Rep.* **9** 1–13
[61] Mueller S and Sandrin L 2010 Liver stiffness: a novel parameter for the diagnosis of liver disease *Hepat. Med.* **2** 49
[62] Chatelin S, Constantinesco A and Willinger R 2010 Fifty years of brain tissue mechanical testing: from *in vitro* to *in vivo* investigations *Biorheology* **47** 255–76